Annu. Rev. Biophys. Biomol. Struct. 1994. 23:731–61

MOLECULAR DYNAMICS SIMULATIONS OF THE GRAMICIDIN CHANNEL

Benoît Roux

Department of Physics, Université de Montréal, C.P. 6128, succ. A, Canada H3C 3J7

Martin Karplus

Department of Chemistry, Harvard University, 12 Oxford St., Cambridge, Massachusetts 02138

KEY WORDS: ion, membrane, transport, ion diffusion, free energy profile

---

CONTENTS

1056–8700/94/0610–0731$05.00

PERSPECTIVE AND OVERVIEW

The ion channel formed by a dimer of the gramicidin A molecule is the model system for studying, experimentally as well as theoretically, the microscopic processes underlying ion movements across lipid membranes. Gramicidin A is a simple linear antibiotic pentadecapeptide produced by *Bacillus brevis* consisting of alternating L– and D–amino acids: HCO-L-Val1-Gly2-L-Ala3-D-Leu4-L-Ala5-D-Val6-L-Val7-D-Val8-L-Trp9-D-Leu10-L-Trp11-D-Leu12-L-Trp13-D-Leu14-L-Trp15-$NHCH_2CH_2OH$. The ion conducting conformation of the gramicidin A channel in a membrane is well established (4, 66, 89, 105). Two-dimensional ^1H NMR in SDS micelles (4) and solid-state ^{15}N (66) and ^{13}C (88) NMR in oriented DMPC bilayers show that the channel is an N-terminal–to–N-terminal (head-to-head) dimer formed by two single-stranded right-handed $\beta^{6.3}$-helices. The dimer is stabilized by the formation of 20 intramonomer and 6 intermonomer $-NH\cdots O-$ backbone hydrogen bonds to form a pore about 26 Å long and 4 Å in diameter. The hydrogen-bonded carbonyls line the pore, and the amino acid side chains, most of them hydrophobic, extend out into the membrane lipid. The structure of the channel is such that the permeation process must involve the single-file translocation of a partially dehydrated ion and water through the interior of a narrow pore.

The channel is permeable to water molecules and to monovalent cations with the selectivity sequence $Li^+ < Na^+ < K^+ < Rb^+ < Cs^+$, which corresponds to their mobility in bulk water; it is impermeable to anions and blocked by divalent cations. Cation binding sites are located at the C terminus of the monomers, near D-Leu10 (67, 88, 97). Monovalent cations partition spontaneously into the channel, but the equilibrium binding constant of the monovalent cations is relatively weak, suggesting that the free energy in the binding site is similar to the chemical potential in bulk water (35). The effective diffusion constants of a water molecule and of a Na^+ in the interior of the pore have a similar order of magnitude and are both much smaller than in bulk solution (see 79). The channel can be occupied by two permeating ions at sufficiently high concentration, and double occupancy is relatively more likely for the larger cations. Chemical modifications of the side chains can influence ion permeation (2, 7) and the stability of the dimer channel in the lipid bilayer (6).

The gramicidin channel provides a tool for studying the fundamental principles governing the properties of ion channels. Comprehending how any ion channel functions from a microscopic point of view, even the one formed by the relatively simple gramicidin molecule, represents

a challenge. Although modern molecular dynamics techniques have been shown to be powerful methods for the study of biological systems of ever-increasing complexity (12), theoretical investigations of ion transport are faced with particularly difficult problems. First, a very accurate model for the interactions involved is necessary. The large solvation-free energies of ions (e.g. around -100 kcal/mol for Na^+) contrast with the activation energies for transport through the channel, deduced from experimentally observed ion-fluxes; they generally do not exceed 10 k_BT (1, 22). This implies that the energetics of ion transport results from a delicate balance of very large interactions. Second, the time-scales involved are long relative to possible simulation times. The passage of one ion across a channel takes place on a microsecond time scale (1, 22, 37), while realistic simulations of biological systems typically do not exceed a few nanoseconds (12). A variety of special computational techniques are necessary to extract information about these slower and more complex processes (12).

Because these difficulties imply that straightforward simulations can supply only limited information about the properties of the gramicidin channel, vastly different theoretical models have been proposed to study the permeation process. The goal of this review is to provide an overview of the theoretical approaches based on atomic models that have been used to study the gramicidin channel and to present our current level of understanding of the channel. Other channel-forming and ion-transport molecules, as well as phenomenological descriptions based on continuum electrostatics (40, 68), barrier hopping models (53), or the Nernst-Planck continuum diffusion equation (57), are not included. The conducting channel properties, such as selectivity, flux, double occupancy, water permeability, competition, and blocking have been reviewed previously (1, 22, 37).

SHORT HISTORY

Theoretical studies of the gramicidin channel at the atomic level started in 1973 with the simplified dipole model of Läuger (53), which was concerned with the basic problem of the rate of ion transport. Since then there has been an evolution in computer power, potential energy functions, ab initio calculations, molecular dynamics simulations, activated dynamics, and free-energy simulation techniques (12). Also, the potential of mean force (PMF), which was introduced by Kirkwood in 1935 (51) for the structure of fluids, has become a central concept in the treatment of transition rates and reaction dynamics in liquids (14), in general, and of ion transport, in particular, and special simu-

lation techniques were developed for its evaluation (for a review, see 12). Similarly, experimental knowledge of the structure of membrane peptides and proteins has progressed significantly. Several of the early theoretical studies were done at a time when there remained some confusion about the microscopic significance of rate theories (for example, see 68a, p. 275) and the validity of the left- or right-handedness of the dimer channel conformation (see 105 for a review).

The oldest and simplest model is the stylized periodic helix, which was introduced in 1981 by Fischer, Brickmann & Läuger (FBL) (30); it dates back to the simple periodic array of dipoles used by Läuger in 1973 (53). In the same period, several realistic models with atomic details were developed independently by Pullman & Etchebest (PE) (74), Fornili, Vercauteren & Clementi (FVC) (31), and Mackay, Berens, Wilson & Hagler (MBWH) (58). The MBWH model, which made use of the recent development of molecular dynamics simulations of proteins (62), had a profound influence on subsequent studies of the gramicidin channel; even though the full paper describing the work never appeared in print, it seems to have had a wider circulation and readership than many published papers. Prior to this model, the channel was represented as a rigid structure fixed in space (PE and FVC; FBL allowed some restricted librational motions). Subsequent to MBWH, the theoretical models developed by Lee & Jordan (LJ) (56), Chiu, Subramaniam, Jakobsson & McCammon (CSJM) (19), Åqvist & Warshel (AW) (3), and Roux & Karplus (RK) (79) all accounted, to varying degrees, for the flexibility of the channel.

Simulations of the full atomic model of the gramicidin dimer in the presence of water and a simplified treatment of the membrane have been used recently for a detailed study of the mechanism of ion transport (81). The next stage in theoretical models of the gramicidin channel includes the phospholipid membrane environment surrounding the channel. Several such studies are in progress (101, 102, 106–108).

MICROSCOPIC MODELS AND COMPUTATIONAL APPROACHES

This section briefly reviews the conformational models used for the gramicidin channel. Acronyms referring to a model are based on the names of the authors of the initial paper (see above). Particular attention is given to the nature of the approximations involved in each model; i.e. the structure used for the channel, the treatment of hydration, the potential functions used, and the computational techniques

employed. An attempt is made to describe results obtained from the various models and to evaluate their validity in light of our present knowledge.

Structural Models

The head-to-head left-handed helical dimer first proposed by Urry in 1971 (96; see also 99), which is now known to be correct in general though of the wrong handedness, was refined by Ventakachalam & Urry (98) using energy minimization techniques with helix symmetry constraints. The flexibility of the structure and the energetics of the peptide libration were examined in another study (100). The potential function used for these studies was based on the ECEPP force field (63) in which the ϕ,ψ dihedral angles are allowed to vary; other internal coordinates (i.e. bond length and angles) are kept fixed. Based on standard peptide geometry, Koeppe & Kimura constructed families of β-helices and proposed a left-handed helical dimer structure (52). No potential energy function was used by Koeppe & Kimura in their work, i.e. the conformation was constructed as a perfect helix from geometrical considerations (above).

Infinite periodic poly (L,D)-alanine β-helices were studied by Roux & Karplus (79), Naik & Krimm (65) and by Monoi (64). Refined left- and right-handed models of the helical dimer were obtained using full geometry optimization with energy minimization techniques. The left-handed RK dimer was obtained from the Ventakachalam-Urry conformation using the CHARMM program (78); the Koeppe-Kimura conformation was refined using GROMOS (CSJM) (19). The CSJM (17) and RK (81) models of the right-handed dimer were obtained by use of experimental NMR data from Arseniev et al (4).

The experimental determination of the structure of the ion-conducting conformation of the gramicidin A channel in a membrane also made use of molecular modeling. The conformation of the right-handed dimer incorporated in SDS micelles was obtained by Arseniev et al (4) from the experimentally determined proton-proton nuclear Overhauser effects (NOEs) observed by two-dimensional NMR, which were used as distance constraints in a geometry optimization (4). The conformation of the backbone and tryptophan side chains of the right-handed dimer in a dimyristoyl phosphatidylcholine (DMPC) bilayer was determined (TA Cross, personal communication) using geometrical constraints based on the chemical shifts and dipolar couplings observed by solid-state NMR of isotopically labeled gramicidin channels aligned parallel to the magnetic field direction (66); the complete determination of the conformation of the other side chains is in progress.

The FBL Model

Fischer, Brickmann & Läuger (FBL) (30) proposed a simplified gramicidin-like model. In this model, the channel is represented by a rigid periodic helical arrangement of dipolar carbonyl groups consisting of two point charges, one for the carbon and one for the oxygen atoms. There are six carbonyl groups per helix turn pointing in alternating directions and located on the surface of a cylinder of radius 3.2 Å. The flexibility due to the carbonyl librational motions is incorporated by allowing limited displacements of the oxygens that result in small variations of the tilt angle of the dipolar group relative to the helix axis.

The simplicity of the FBL helix made it an attractive computational model for illustrating formal theoretical developments. For example, Läuger used it in 1982 (54) to calculate the PMF of an ion constrained on the axis of the FBL helix model by means an explicit numerical integration of the partition function. Most of the early molecular dynamics simulations of the FBL helix were reviewed by Polymeropoulos & Brickmann (72). In the later studies by Skerra & Brickmann, molecular dynamics simulations of Li^+, Na^+, and K^+ were performed in the FBL helix in the presence of explicit water molecules to investigate the structure and dynamics of one-dimensional ionic solutions (86) and the effect of voltage on ion diffusion (87; see also 84). The interaction of the ions with the helix atoms were represented in terms of partial-charge electrostatics and Lennard-Jones potentials. The TIP4P water-water potential was used for the explicit water molecules (45). The total number of waters included varied from six to nine. The ion mobility was extracted from the average drift in the presence of an external potential (87).

The PE Model

Pullman & Etchebest (PE) (74) developed a model in which the channel is represented in detail by a rigid polyglycine analogue of the left-handed helical dimer. The side chains were omitted except in one study (23). Solvent was considered but no membrane environment was included.

Because the channel is rigidly fixed in space, the potential energy concerns only the nonbonded ion-water, ion-peptide, water-water, and water-peptide interactions. One notable feature of the PE model is the nature of the molecular mechanism's potential function; it is based entirely on ab initio calculations. The interactions are described as a sum of terms including an electrostatic multipole expansion, van der

Waals dispersion effects, overlap repulsion, charge transfer and first-order induced polarization (33).

Several studies were done using an approach that relied mostly on the analysis of optimized configurations obtained from energy minimization techniques. In particular, adiabatic energy profiles were calculated by fixing the ion at various position along the channel axis and optimizing the configuration of the channel system. Because it is extracted from energy minimized configurations, an adiabatic energy profile does not account for thermal fluctuations and, thus, corresponds to a zero-Kelvin approximation to the PMF.

The approach based on the calculation of adiabatic energy profiles was used to investigate the energetics of Na^+ in the singly and doubly occupied channel without (74) and with (24, 25, 75) water, the influence of the flexibility of the ethanolamine tail (28), the influence of side chains (23, 34), the influence of handedness, the binding of Ca^{2+} (29), and the energy profile of Cs^+ with water (27; for a review, see 73).

In all the studies [except the one concerned with the handedness of the channel (26)] the structure of the channel was rigidly fixed in the left-handed Urry dimer conformation (99). The optimization of only a limited number of degrees of freedom was considered in each, such as the influence of the isomerization of the ethanolamine tail. A few water molecules (16 to 24) were included in the single-file region and at the channel entrance to study the effect of dehydration (24, 25, 75).

The FVC Model

In the model developed by Fornili, Vercauteren & Clementi (FVC) (31), the channel is represented as a rigid left-handed structure including all the backbone and side-chain atoms. Because the channel is rigidly fixed in space (as in the PE model), the potential energy concerns only the nonbonded ion-water, ion-peptide, water-water, and water-peptide interactions. All nonbonded interactions were described in terms of Lennard-Jones and partial charge electrostatics with 6-12-1 radial functions; the parameters were obtained by fitting ab initio calculations. The hydration was taken into account explicitly by including 80 water molecules inside a cylindrical volume. During the simulations, the waters were constrained to stay within the cylindrical volume, and a translational symmetry constraint was imposed along the channel axis (periodic boundary conditions) (50). The MCY potentials were used for the water-water interactions (60). The membrane environment was ignored.

The model was used in Metropolis Monte Carlo simulations of the waters and cation at 300 K in the presence of the fixed channel structure. Average potential energy profiles were calculated and analyzed in terms of the various contributions for fixed positions of the cations along the channel axis. The water structure (31) and the energetics and hydration shell structure of Li^+, Na^+, and K^+ inside the channel were examined (49, 50). A related study of the effect of voltage on Na^+ and K^+ was made by Kim using the FVC model (48); a voltage difference of 500 mV was applied over a distance of 32 Å. The reorientation of the water molecule due to the applied voltage was analyzed, and the average potential energy was calculated for different ion locations along the channel axis.

The MBWH Model

In the model developed by Mackay, Berens, Wilson & Hagler (MBWH) (58), the channel is represented as a fully flexible left-handed Urry-like structure that includes all the atoms of the backbone and of the side chains (552 atoms). The potential function consisted of terms for bonds, angles, and dihedral angles; nonbonded interactions were described with a Lennard-Jones term and a term for the Coulombic interactions (details in 58).

The MBWH model was the first to include the full flexibility of a realistic representation of the gramicidin molecule based on a molecular dynamics simulation. The simulations were used to study the structure and dynamics of water and cations (Li^+, Na^+, K^+, and Cs^+) inside the channel (58, 59). Thirteen waters were included to provide the primary hydration in the single-file region; the SPC water model was used (8). One water was replaced by a cation for the one monomer-centered and dimer-centered ion position. The monovalent cations Li^+, Na^+, K^+, and Cs^+ were studied. The simulations were relatively short, 5 ps in the initial study of the cation systems (58) and 30 ps for the water-filled channel (59). Qualitative observations were made concerning the structure and dynamics of a flexible gramicidin channel, the single-file structure of the internal waters, and the deformation of the backbone in the presence of a cation.

In an ambitious investigation, never published but reported by Jordan (41), Mackay, Edelsten & Wilson calculated the free energy of materialization of a Cs^+ ion at five different locations along the channel axis by using free-energy simulation techniques. The model system included 1 gramicidin dimer channel, 8–10 waters filling the channel interior, and 90 waters at the pore's openings, representing the bulk-water interface. A translational symmetry constraint was imposed along the

channel axis (periodic boundary conditions). The membrane environment was ignored.

The RK Models

THE RK-HELIX Roux & Karplus developed a periodic poly (L,D)-alanine β-helix gramicidin-like model to investigate the translocation mechanism in the interior of the gramicidin A channel (79, 80); the side chains of gramicidin were neglected to simplify the system and introduce periodicity. The approach is reminiscent of the FBL helix, although the atomic representation of the structure is more realistic. The microscopic interactions and the potential functions were based on a polar-hydrogen representation of the system, in which all heavy atoms and all polar hydrogens (those able to form hydrogen bonds) are included; the aliphatic hydrogens are treated as part of the carbon to which they are attached. The model used TIP3P water (45), and peptide-peptide and water-peptide potential functions from the CHARMM (11). Special care was given to the parametrization of the interaction of the ion with the channel and water. The potential was developed from ab initio calculations of the interactions of sodium with water and of sodium with acetamide and *N*-methylacetamide; the latter were chosen as models of the carbonyl group of the peptide backbone (79). First-order polarization induced by the ion on the peptide was included. All degrees of freedom were allowed to vary except the bonds involving the polar hydrogens, which were constrained to a fixed length.

The PMF of Na^+ and K^+ along the axis of the periodic helix were determined with the free-energy perturbation difference technique (79). An integrated mean force decomposition was used to analyze the important contributions to the PMF (79). Based on this formulation, the mean force is decomposed linearly to obtain the various contributions to the PMF along the reaction path. The transport properties of water, Na^+, and K^+ in the periodic β-helix were investigated with methods appropriate for each of these species. For water, the mean-square displacement was determined from a simulation; for Na^+, an activated dynamics approach was used; and for K^+, the response to an external field was analyzed (80). The transmission coefficient and the deviation from transition state theory were estimated from the Na^+-activated dynamics trajectories. A cross-coupling friction decomposition method was used to analyze the factors contributing to the total friction acting on ions. The instantaneous deviation of the force is decomposed into a sum of contributions to obtain information about the underlying fac-

tors giving rise to the friction coefficient, as is done in the integrated mean force decomposition method.

THE RK DIMER Roux & Karplus (78) developed a model of the helical dimer embedded in a model membrane, including all the side chain atoms. To produce a hydrocarbon-like membrane environment and to prevent waters from reaching the lateral side of the dimer, a model membrane made up of Lennard-Jones spheres corresponding to the size of a CH_3 group was included. The entrance of the channel was fully solvated by 190 water molecules. Periodic boundary conditions were applied along the channel axis. A cylindrical confining potential was applied in the radial direction on the water oxygens to maintain the proper density in the bulk-like regions of the system. The system consists of 314 peptide atoms for the gramicidin dimer, 190 water molecules and 85 "membrane" spheres. The model also employed the same polar hydrogen representation and potential function as used for the periodic helix.

In a first study, a system was constructed with the left-handed helical dimer conformation embedded in the model membrane to study the dynamics of water in the interior of the channel (B Roux & M Karplus, unpublished calculations; see also 76). In a second study, the PMF of Na^+ along the dimer axis was calculated using a free-energy perturbation difference technique (81); the method is the same as that used for the periodic helix model. The reaction coordinate was defined as the projection of the ion position onto the vector joining the centers of mass of the gramicidin monomers. The channel was constructed as a right-handed head-to-head helical dimer from the coordinates of the Arseniev structure (4). Three regions were investigated in detail: the monomer-monomer junction, the beginning of the single file, and the dehydration step at the entrance. The main results are shown in Figure 1 (below). The position of the binding site was determined (see Table 1, below). The solvation properties of the single-file region, the dehydration process at the entrance of the channel, and the translocation barrier at the monomer-monomer junction were analyzed. These results were combined with those from the periodic helix to obtain an estimate of the potential of mean force acting on the ion throughout the entire channel.

Organic Ion Models

The extended atom RK dimer model, based on the CHARMM force field (11) was used by Busath et al (13), and by Turano et al (95), to study the permeation of large organic ions. The adiabatic energy profiles of guanidinium, acetamidinium, and formamidinium were calcu-

lated, i.e. the configuration of the channel and of the ion was optimized using energy minimization techniques for restricted position of the ion along the channel axis. The organic cation structures and parameters were derived from the standard CHARMM arginine side chain. No water molecules were included.

The CSJM Model

Chiu, Subramaniam, Jakobsson & McCammon (CSJM) (19) developed a model of the helical dimer including all the side-chain atoms in an extended atom representation using the standard GROMOS force field and dynamics program (100a). In most studies, the channel was constructed as a right-handed helical dimer (15, 16, 18); a left-handed structure was used initially (19). An artificial nonelastic time relaxation restraint was applied directly to the helix atoms to mimic the influence of the surrounding lipids and to maintain the helical dimer in the neighborhood of the Koeppe-Kimura model-built structure (52).

To introduce the solvent in the single-file region in the interior of the channel, approximately 23 waters were included in the first simulation (19); the SPC water model was used (8). The number was increased to 109 in later simulations to provide a bulk-like region at the mouth of the channel; the bulk waters were maintained as hemispherical caps with a cube-shaped boundary potential (15, 16, 18).

The CSJM model was used in several molecular dynamics simulations to study the correlated motions of water molecules in the channel (16, 19), to compare the average structure with that deduced from solid state NMR data (17), to study the side-chain conformations in vacuum (15), and to examine the displacement of a Na^+ in the interior of the channel (18). The motions of water and ion were analyzed in terms of time-correlation functions. The translocation barrier of Na^+ in the interior of the channel was estimated by interpreting the mean-square-displacement of the center of mass of the ion-water complex in terms of a Langevin equation (18).

The LJ Model

The model developed by Lee & Jordan (LJ) (56) represents the channel as a polyglycine analogue of the Urry left-handed helical dimer. The formyl and ethanolamine end groups are included and the side chains are neglected.

The potential function used differs significantly from the more common biomolecular force fields such as used in MBWH, RK, and CSJM. The influence of polarization is treated explicitly and the polarization is calculated self-consistently by an iterative method (56; see also 44).

The basic peptide dynamical units are uncharged dipolar polarizable groups (CO and NH), rather than individual atoms with partial charges (C, O, N, and H). It is possible that the parametrization of the potential is not optimal for protein simulations (44); the hydrogen bonds of the dimer were not stable and it was necessary to add a peptide group localization energy term (an artificial harmonic restraint) to maintain the helical structure.

The LJ model was used in a series of studies to investigate cation motions (56), valence selectivity (91, 92), the properties of different channel conformations (93, 94), and the permeation process of Cs^+ (41–44). Few waters were included in the initial investigations (56), and the polarizable electropole water model of Finney and coworkers was used (5). In the most recent investigations (43, 44), the PMF of Cs^+ was calculated using umbrella sampling (70). The channel was embedded in a model membrane of 589 hydrocarbon-like CH_2 spheres. In the calculations, bulk water was approximated by hemispherical regions with an 18-Å radius at each end of the channel; 419 water molecules were included (44). Thus, the overall system is constructed similarly to that of RK, although very different potential functions are used.

The AW Model

The model developed by Åqvist & Warshel (AW) (3) was used in a single study of the PMF of Na^+ along the channel axis. The channel is represented as a polyglycine analogue of the left-handed helical dimer including the formyl and ethanolamine end groups; the side chains were neglected. The peptide-peptide potential function was taken from Warshel & Levitt (103). Special care was given to the treatment of the long-range electrostatic interactions with the hydrocarbon membrane region. The channel was embedded in a model hydrocarbon membrane environment represented by a cylindrical region containing a polarizable cubic lattice with a dielectric constant of 2. The Lennard-Jones parameters for the Na^+ ion were fitted empirically to reproduce the experimental free energy of solvation of Na^+ in water.

The free energy of the alchemical transformation of a Na^+ ion into a water molecule was calculated explicitly for two ion locations along the channel axis with the free-energy perturbation molecular dynamics simulation technique. Twenty waters were included. To obtain the free energy relative to that of bulk water, the transformation was made both in the channel and in a bulk water environment. The methodology to determine the other points of the PMF along the channel axis was based on the protein dipole Langevin dipole (PDLD) approach, in which explicit waters are replaced by dipoles located on a cubic grid, and only

two waters were treated explicitly. The remaining waters of the single-file region, as well as the bulk water, were represented by the PDLD approach. Problems may occur with the approximation near the entrance of the channel, as the Na^+ and the two single-file waters leave the interior of the channel and enter the bulk water region described by the lattice (see Figure 2 in Ref. 3). In constructing the grid, the PDLD dipoles overlapping with the ion core are excluded (those within a distance of 2.4 Å). The exclusion distance has a role similar to the ionic radius in the Born model of solvation (10). The PDLD approach is similar in spirit to approximate solvation models based on continuum electrostatics, such as the Poisson-Boltzmann equation (32), although the dielectric medium here is represented by discrete dipoles on a grid. Thus, the AW calculation uses a mixed method involving both atomistic and phenomenological representations of matter.

MAIN RESULTS

Channel Conformation

Distorsion of the ideal β-helical symmetry, which was excluded in the Ventakachalam-Urry (98) and Koeppe-Kimura (52) models, has been observed in models accounting for the full flexibility of the structure (17, 44, 78). The mouth of the channel is deformed and slightly constricted in the CHARMM-based (11) RK-dimer model (13, 76, 78, 95), while it is closer to an ideal helix in the GROMOS-based (100a) CSJM model (17). The deformations at the channel ends were attributed to a break in the hydrogen-bond network of the helix due to the inward bending of the carbonyl oxygens of Trp13 and Trp15 (13, 76, 78, 95) or to side-chain steric interferences (17).

The CSJM (17) and RK (81) models of the right-handed helical dimer conformation were compared to the structure determined by solid-state NMR (T Cross, personal communication; see also 17). It is found that the overall structure of both models is in very good agreement with the experimental data. However, careful analysis of the NMR results suggests that finer details of the backbone conformation, in particular small deviations from planarity of the peptide linkage near the channel mouth, may not be correctly reproduced.

Structure and Dynamics of Single-File Water

Several studies of the structure and dynamics of the single-file waters have been made because they represent a very interesting feature of this channel and might be of significance for extended water chains in

the interior of some proteins (e.g. the existence of water chains in the interior of bacteriorhodopsin has been proposed). Analyses have been made by CSJM (19, 16), PE (24, 25, 75), FVC (31), LJ (44), MBWH (58, 59) and RK (76, 80). Given the considerable variations in the theoretical approaches, the calculated properties of the water structure inside the channel are remarkably consistent. Most simulations resulted in 8–10 water molecules in the single-file region, in qualitative agreement with experiments (1). In the channel interior, the water molecules always form essentially linear hydrogen-bonded chains with the water hydrogens interacting preferentially with the oxygens of L-carbonyl groups and the ethanolamine end in the PE model (in the left-handed helical dimer) (24, 25, 75). There are, however, some differences among the theoretical results. This indicates that certain aspects of the hydrogen-bonded water chain are sensitive to the details of the microscopic models, including the choice of the potential function. The FVC (31), PE (24, 25, 75), MBWH (58, 59), RK-helix (79, 80), and CSJM (19, 17) models resulted in configurations in which the water molecules in the interior of the channel point in the same direction along the channel axis. In contrast, the single-file water chain does not show persistent orientational correlations propagating through the whole length of the channel in the more realistic RK-dimer model (76) and in the LJ (44) models. Gaps and defects, breaking the continuous hydrogen-bonded water chains, have been found, and it is possible that the perfect single file of water molecules is interrupted over significant time intervals. In fact, a closer examination of the results reported for CSJM (19) and FVC (31) reveals that noncorrelated linear structures, in which all water molecules do not point in the same direction, occurred in the simulations, though they were infrequent. The dynamics and mobility of the water molecules along the axis of the dimer channel also differ. The calculated diffusion constants, 6×10^{-6} cm^2/s (17) and 2.5×10^{-7} cm^2/s (76), do not differ significantly from that estimated from the experimental water permeability: 4.4×10^{-7} cm^2/s (see 79). The diffusion constant of water molecules inside the channel is reduced relative to its value in bulk water both in the simulations and from experiment; i.e. in bulk water, the experimental value is 2.1×10^{-5} cm^2/s, and molecular dynamics yields 3.2×10^{-5} and 3.7×10^{-5} cm^2/s for TIP3P and SPC, respectively (17, 79).

The dynamical properties of the single-file water chain were found to be affected by the strength of artificial restraints on the backbone conformation (17); i.e. the translational mobility of the single-file waters is facilitated by peptide motions and is dramatically reduced by holding the channel rigid. The tendency of the oxygen of the water

molecules in each monomer to point towards the bulk solution at the N-terminus has been related to an increase in the water-carbonyl interactions at the mouth of the channel that result from the helical distortion and pore constriction at the termini (76); the constriction makes the carbonyl at the termini more accessible for hydrogen bonding with the single-file water molecules. The orientation of the waters at the termini, in the absence of an ion, has been attributed to the interactions with the carbonyl groups in the channel mouth (44).

The properties of the single-file water configuration are very sensitive to the water-water and water-peptide potential energy functions (58); decreasing the water-backbone hydrogen-bonding interactions by 5% altered the single-file structure significantly; it caused some of the waters to leave the pore. Generally, the water models used, i.e. the MCY water model (60) used in FVC, the SPC water model (8) used in MBWH and CSJM, the TIP3P water model (45) used in RK, and the TIP4P water model (45) used in FBL (86, 87), are all based on pairwise effective nonpolarizable, Lennard-Jones partial charge electrostatic, 6-12-1 potential functions. The SIBFA waters (33) used in PE, and the polarizable electropole water model (5) used in LJ are significantly different. The SPC, TIP3P, and TIP4P models were parametrized to reproduce the properties of bulk water; the SIBFA and MCY waters were developed from ab initio potentials; the polarizable electropole water model was adjusted to reproduce several properties of small water clusters (5). Incorporation of polarizability markedly affects the properties of the single-file water (44); the average induced dipole of the single-file waters (2.31 Debye) is smaller than in bulk water (2.47 Debye). In comparison, the nonpolarizable TIP3P waters have a fixed dipole of 2.35 Debye (45). Thus, whether the most widely employed water models realistically describe the energetics of the single-file water molecules in the confined environment of a pore is uncertain.

Energy Profiles

Several studies were concerned with the mapping of the adiabatic energy profile along the permeation pathway (see all the PE studies). Others have considered the thermally averaged potential energy profile of ions and water inside the channel (e.g. see all FVC references) (56). These quantities, although of considerable interest, do not provide a direct link with the modern statistical mechanical theories of dynamical rate processes in liquids (9, 14). Furthermore, the rigid channel structure used in the PE and FVC studies introduce artifacts because the flexibility of the backbone is important (58, 78, 79, 81). Thus, except for some structural features, such as the position of the stable energy

wells (see below), these early results are not truly comparable to the PMF calculations performed subsequently.

Four calculations of the PMF of ions along the axis of the gramicidin channel have been reported: (*a*) DH Mackay, PM Edelsten & KR Wilson calculated the PMF for Cs^+ along the axis of a left-handed dimer (MBWH model) (unpublished calculation reported in 41); (*b*) Åqvist & Warshel calculated the PMF of Na^+ along the axis of a polyglycine left-handed dimer using an alchemical transformation technique (AW model) (3); (*c*) Jordan calculated the PMF of Cs^+ along the axis of a polyglycine left-handed dimer using umbrella sampling (LJ model) (44); (*d*) Roux & Karplus calculated the PMF of Na^+ along the axis of a right-handed dimer channel embedded in a model membrane using a free-energy difference perturbation technique (RK dimer) (81). The last investigation (*d*) was the only one that used the known experimental right-handed dimer channel conformation, and at present it is the PMF calculation that is based on the most realistic gramicidin model. Other studies provide closely related information about the translocation barriers in the interior of the channel. Roux & Karplus calculated the PMF of Na^+ and K^+ along the axis of a periodic helix (RK helix) using a free-energy difference perturbation technique (79). A study by Chiu et al (18) provided information related to the PMF of Na^+ (CSJM model). The translocation free-energy barrier was estimated from the mean-square-displacement time correlation function. Skerra & Brickmann studied the translocation rate of ions along the axis of a periodic helix (FBL) (86, 87).

Although the results are qualitatively reasonable, there are quantitative problems. Most calculated activation free-energy barriers are too large compared with experimental estimates (44, 81; see also DH Mackay, PM Edelsten & KR Wilson, unpublished calculation reported in 41); e.g. the largest barriers for Na^+ found by RK are in the range of 8–12 kcal/mol, while experiments suggest an upper bound on the order of 5–10 kcal/mol (1, 22). In several calculations, the ion was more stable in bulk solution than inside the pore (3, 44). Imbalances of the large ion-water and ion-peptide interaction energy are probably responsible for the overestimated activation barriers. An important test of the potential functions is provided by calculations on small model systems which can be compared directly with experimental data. For example, in the gas phase the ion-water interaction is 34, 24, and 18 kcal/mol for Li^+, Na^+, and K^+, respectively (46); the corresponding interaction with dimethylformamide, taken as a model of the carbonyl peptide group, is 51 kcal/mol for Li^+ (90), 38 for Na^+ from ab initio calculations (see 79), and 31 kcal/mol for K^+ (47). Standard biomo-

lecular force fields, such as those used in several models (FBL, FVC, MBWH, CSJM, AW, and TPB), can lead to a significantly underestimated ion-peptide interaction; e.g. an affinity of 32 kcal/mol for Na^+ and dimethylformamide is found instead of the correct value of 38 kcal/mol (B Roux & M Karplus, unpublished results). Polarization and nonadditive effects may also be important (77, 82). Nevertheless, the results share some interesting features that are described below.

On a methodological note, simulation techniques based on small local free-energy differences in the neighborhood of a sequence of reference ion positions, such as umbrella sampling (43, 44), free-energy difference perturbation, or integrated mean force (79, 81), appear to be most appropriate for calculating the PMF. An important problem with the materialization (41) or alchemical transformation (3) techniques is that the PMF along the axis of the channel is extracted from small variations of a large number. For example, the absolute free energy of a Na^+ at any position x along the channel axis is approximately 100 kcal/mol, whereas the PMF is expected to have variations smaller than 5 kcal/mol. The advantages of the approach used by Chiu et al (18), which was based on an interpretation of the mean-square displacement in terms of a Langevin equation, over more standard techniques are unclear because time correlation functions have a larger statistical error than equilibrium averages (55). With all the free-energy techniques, it is necessary to perform long simulations to avoid hysteresis effects (79, 81). Such sampling bias, caused by a lack of equilibration, has also been observed in free-energy calculations in bulk water (61).

ION BINDING SITES The free-energy profile of Na^+ along the axis of the right-handed dimer channel calculated by Roux & Karplus is shown in Figure 1 (below). The main binding site was found 9.3 Å from the center of the channel, where the Na^+ is bound to D-Val8, D-Leu10, L-Trp13, and L-Trp15, in good agreement with experimental observations (67, 88, 97). The binding sites are located in the single-file region, where the ion is in close contact with four carbonyl oxygens and two water molecules.

Jordan has found a stable position for a Cs^+ around 9.0 Å in a left-handed dimer, although this position did not correspond to a global free-energy minimum (44); the most stable position was found around 13.5 Å, where the ion maintains most of its hydration. The most stable position found by Åqvist & Warshel was around 14.0 Å, outside the single-file region of the channel. However, because their calculation was based on the approximate PDLD method and includes only two waters explicitly, the significance of the free-energy profile at the en-

trance of the channel, where the Na^+ is only partly dehydrated, is not clear (see the section on the AW model, above); Na^+ is still directly coordinated by three to four waters at 14.0 Å in the right-handed helix (81).

The PE adiabatic energy profile and the FVC average potential energy, which were based on energy calculations with rigid structures, have their deepest minimum for Na^+ at 4.5 Å, inside the single-file region, and at 15 Å, outside the channel. However, rigid structures do not give a valid representation of the inward deflection of the C=O carbonyl in the presence of an ion (58). Ion-carbonyl interactions and the local flexibility of the backbone are essential factors giving rise to the binding site around 9.3 Å (81).

ELEMENTARY TRANSLOCATION BARRIER IN THE INTERIOR OF THE CHANNEL Based on the calculations of Roux & Karplus (81), a sequence of small free-energy barriers oppose the movements of the permeating cation in the interior of the channel, where a hydrated complex must translocate in single file. The principal energy barrier is at the entrance of the channel, at the beginning of the single-file region. The small barriers, superimposed on the more global features of the PMF (see below), are due to the association of the ions with individual carbonyls along the channel axis. In the single-file region, the Na^+ is coordinated by four carbonyls and two water molecules. The magnitude of the translocation barrier is 4–5 kcal/mol, with a slightly smaller barrier at the monomer-monomer junction. Other estimates for the elementary Na^+ translocation barrier inside the pore are 3.5 kcal/mol (56), 4–5 kcal/mol (3), and 3.2 kcal/mol (18). The effect of handedness is expected to be small in the channel interior. Consequently, it is possible to compare results obtained for left- and right-handed helices for the translocation mechanism inside the pore, away from the ends and the monomer-monomer junction (79) (see also the section on channel conformation, above).

The structural and energetic aspects of the elementary translocation steps of Na^+ in the interior of the pore were investigated in more detail with the periodic RK-helix (79). Two residues form the basic building block and the system is expected to have a periodicity of 1.55 Å. It follows that the PMF along the axis of the RK-helix is made up of a sequence of well-defined binding sites and energy barriers separated by 1.55 Å; there is one such local well for every (L,D) pair of carbonyl oxygens. These results for the periodic helix can be compared with the relative minima in the PMF for Na^+ obtained for the full dimer channel model. Minima (81) are observed at 6.20, 7.75, 9.30, and 10.85 Å in

the entrance region and at 0.0 and 1.65 Å in the dimer contact region. Thus, the positions of these minima corresponds approximately to integer multiples of 1.55 Å (n = 0, 1, 4, 5, 6, 7), i.e. the length of the helical unit in the periodic RK-helix. For Na^+, the right-handed dimer channel has 15 such local free-energy minima (see Table 1, below). The pattern of ion-carbonyl contacts in the local minima is an attribute of the β-helix structure. A Na^+ is in close contact with carbonyls i, $i+2$, $i+5$, and $i+7$, where i corresponds to the number of and L-amino acid for a left-handed helix and to the number of a D-amino acid for a right-handed helix. For example, Åqvist & Warshel reported local energy minima with carbonyls 3, 5, 8, and 10, and 7, 9, 12, and 14 from calculations of a Na^+ in a left-handed helix, which is entirely consistent with this analysis.

The magnitude of the free-energy barrier for the elementary translocation is a decreasing function of the ion radius. Roux & Karplus compared Na^+ and K^+ and found a reduction of the activation free energy from 4.5 for Na^+ to 1.0 kcal/mol for K^+ in the interior of the pore (79). Using the free-energy perturbation method, it was shown that for a fictitious ion with a radius intermediate between Na^+ and K^+ the barrier is between 2 and 3 kcal/mol. This is in accord with the results of Jordan, who found that the free-energy profile of a Cs^+ is completely uniform in the interior of the channel (44). Similar observations were also made from studies based on the rigid channel models (FVC and PE). Several investigations led to the conclusion that the stronger association of smaller cations with the carbonyl oxygens is an important factor in the larger elementary translocation barrier (28, 56, 58, 79). In the interior of the channel, Li^+ and Na^+ tend to be significantly off-axis at the minima, while the larger ions are closer to the center (58). Also, larger ions produce less distortion of the β-helix hydrogen bonding network, which contributes to the reduction of the free-energy barrier (79). Such results are qualitatively consistent with the selectivity sequence of the gramicidin channel and the greater ionic conductance for the large cations (1, 22).

In contrast with the results of most calculations, Skerra & Brickmann reported that the translocation barrier for Na^+ was much smaller than for Li^+ and K^+ in the FBL helix (87). As a result, the mobility of cations did not increase with the ion size and the correct selectivity sequence was recovered by adjusting the number of water molecules in the channel.

The integrated mean force decomposition method was used to show that the water and the channel make approximately equal contributions to the activation free energy of Na^+, but that only water contributes

to the activation free energy of K^+ (see Figure 2, below) (79). Also, it was found that there is an increase in entropy at the transition state, which is associated with the larger fluctuations of the more loosely bound ion. The free-energy profile of ions is not controlled by the large interaction energies involving the ion (i.e. ion-water and ion-peptide), but rather by the weaker water-water, water-peptide, and peptide-peptide hydrogen bond interactions. This conclusion is fundamentally different from that of previous approaches to the study of ion selectivity in channels, in which the channel structure was essentially rigid, and the ion-channel interaction energy was thought to be the controlling factor in ion selectivity (e.g. in the PE and FVC models).

LIMITATIONS OF THE CONTINUUM MODEL Early applications of continuum electrostatic approximations to membrane transport (40, 68) were inspired by the success of the Born model of ion solvation (10). It was argued that the main cause of the free-energy barrier for crossing the channel arises from from the fact that the membrane region (low dielectric constant) provides a less favorable environment than bulk water (high dielectric constant) (40, 68). This interpretation has been given the name the *image-charge* energy barrier, from the mathematical technique that is used to solve the continuum electrostatic problem for the channel and membrane (see 40).

The importance of such image-charge contributions to the highest free-energy activation barrier observed for Na^+ at $x = 7$ Å along the axis of the right-handed dimer channel was investigated with the integrated mean force decomposition (81). It was found that the long-range electrostatic interactions of the continuum-like farthest bulk and channel water molecules, i.e. those that are not in direct contact with the ion (eight water molecules are in the channel and the others are in the bulk region), have the opposite effect of that expected from the continuum electrostatic models. As expected, the average force arising from the bulk region tends to attract the ion outside the channel. However, this effect is more than compensated by the significant attractive forces arising from the electrostatic interactions with the eight water molecules pointing toward the ion inside the channel. Because the orientational freedom of the water molecules inside the channel differs from bulk water (i.e. they are all oriented in one direction), a continuum electrostatic approximation based an isotropic dielectric constant does not account for the directionality induced by the pore environment. Interpretations based on continuum electrostatics do not account for the discrete nature of the water molecules inside the single-file region (69) and the increased solvation capacity of a linear solvent structure

(58). The increased understanding of ion solvation obtained from detailed simulations has clarified the significance of molecular effects and the limitations of continuum approximations for this system (36, 39, 71, 83).

DEHYDRATION STEP Because of the narrowness of the pore, a permeating ion must exchange the first hydration shell waters for backbone carbonyls in entering the channel. Roux & Karplus (81) observed that the transformation from bulk to single-file solvation of Na^+ is progressive and takes place over a distance of approximately 5 Å between 15 to 10 Å from the center of the dimer; Jordan (44) noted that the number of waters in the first coordination shell of Cs^+ decreased from five to two between 13.7 and 9.5 Å from the center of the dimer. The dehydration of Na^+ and Cs^+ proceeds similarly in the energy minimization calculations of Etchebest & Pullman (26, 73). Association of Na^+ (28, 81) and Cs^+ (44) with the ethanolamine tail was also observed in these calculations.

However, although the structural features of the dehydration process are similar, the calculated PMF differ markedly. Roux & Karplus (81) found no sharp free-energy barrier at the entrance of the channel; the magnitude of the ion-channel interactions is sufficient to compensate for the loss of favorable interactions of the Na^+ with the bulk water molecules. In contrast, dehydration results in a large entrance barrier of almost 20 kcal/mol in the calculation by Jordan (44). The large entrance barrier may be due to an imbalance of the ion-water and ion-peptide interactions of the potential energy function based on groups rather than individual atoms; estimated corrections for the differential effects caused by the cut-off errors and the polarization of the hydrocarbon membrane region could not reduce the entrance barrier by more than 5 kcal/mol.

Other Ions

The permeation of ions other than the five common monovalent cations has been addressed in some studies. Etchebest & Pullman (29) examined the potential energy profile for the entry of a divalent cation, Ca^{2+}. The very low permeability and the blocking effect of this divalent cation was attributed to a deep and narrow potential energy minimum at 10.5 Å. Sung & Jordan (41) studied the potential energy profile of an anion, Cl^-. The experimental observation that this anion neither permeates nor blocks the channel was attributed to a large barrier found at the entrance of the channel (41). Turano et al (95) examined the applicability of the size-exclusion concept for the selectivity of the

gramicidin channel. They studied the permeation of large organic cations such as guanidinium, acetaminidium, and formamidinium. Using full energy minimization of the cation-channel system, they showed that the channel can accommodate the passage of formamidinium with a small energy barrier, but that a significant residual barrier remains for guanadinium and acetaminidium. The residual barrier results primarily from the disruption of the hydrogen-bonding network of the channel and could provide an explanation for the measured selectivity of gramicidin for formamidinium over guanadinium.

Dynamical Factors

Using activated dynamics trajectories, Roux & Karplus (80) estimated that the translocation rate for Na^+ is $2.3 \times 10^8\ s^{-1}$, which corresponds to an effective diffusion constant of $0.55 \times 10^{-7}\ cm^2/s$. From the mean displacement in the presence of an applied voltage, Skerra & Brickmann (87) estimated the mobility of Li^+, Na^+, and K^+ and found that the calculated mobilities varied with the number of waters present in the FBL helix; a value of $0.58 \times 10^{-5}\ cm^2/s$ was found for Na^+ with seven waters. Chiu et al estimated the translocation rate of the sodium-water chain complex to be $6.25 \times 10^9\ s^{-1}$, which corresponds to an effective diffusion constant of $0.94 \times 10^{-6}\ cm^2/s$. Based on the measured saturated maximum sodium conductance (14.6 pmho), the effective diffusion constant in the interior of the pore is approximately $0.94 \times 10^{-7}\ cm^2/s$ (see 80), in reasonable agreement with the result of the RK simulation.

Roux & Karplus (80) analyzed the dynamical factors controlling the movements of Na^+ and K^+ in the interior of the channel. By use of the cross-coupling friction decomposition method, it was shown that water-water, channel-channel, and water-channel cross-coupling contribute equally to the total static friction acting on Na^+ in the interior of the channel. In contrast, the friction acting on K^+ in the interior of the channel is controlled by rapidly fluctuating water forces. The importance of the water-channel cross-coupling contribution in the case of Na^+ suggests that the ion-ligand complex is more tightly structured than in the case of K^+. The motion of Na^+ at the transition state is controlled by local interactions arising from collisions with the neighboring carbonyls and the two nearest water molecules. The motion of K^+, in contrast, is controlled by the diffusion of water. Both Na^+ and K^+ suffer many rapid collisions; their dynamics are overdamped and noninertial. Consequently, the selectivity of ions in the β-helix is not influenced strongly by their mass. This contradicts the mass-dependent transition state theory of Schroeder et al (85).

As described above, the PMF of Na^+ is composed of a sequence of small free-energy barriers and the the translocation proceeds in terms of an activated hopping process between discrete states, as in classical transition-state models. However, classical transition-state theory does not provide an adequate picture of the dynamics of ions in the interior of the channel and overestimates the exact rate by one order of magnitude (80). The calculated transition state–theory rate for Na^+ in the RK-helix was $2.1 \times 10^9\ s^{-1}$. To account for the collisional recrossings and dynamical dissipative processes taking place at the transition state (9), the transition state–theory rate must be multiplied by the transmission coefficient. The transmission coefficient, calculated using activated dynamics techniques is 0.11 (80). A high friction approximation for the transmission coefficient of Na^+ gives 0.08. The latter value is in close agreement with the transmission coefficient obtained by Chiu et al (18) from their molecular dynamics trajectory based on an analysis in terms of an approximate Langevin equation. The transmission coefficient is not as small as predicted by the high friction approximation because of inertial non-Markovian dynamical factors (80). Since the dynamics at the barrier top is controlled primarily by high-frequency fluctuations, the transmission coefficient of Na^+ is insensitive to the full static friction assumed in the high friction approximation. However, the high friction approximation provides a better estimate than classical transition-state theory. In the case of K^+, the PMF does not have a large activation barrier and the translocation proceeds in terms of continuous diffusion, as in the Nernst-Planck diffusion approximation. Here the high-friction limit is appropriate.

CONCLUSION AND CRITICAL DISCUSSION

The results of the molecular dynamics calculations with the right-handed dimer channel (81) and with the periodic β-helix (79, 80) provide an understanding of ion transport through the gramicidin channel. The PMF of Na^+ along the axis of the dimer channel consists of a sequence of 15 small free-energy wells, one for every (L,D) pair (see Figure 1 and Table 1). The deepest minimum along the PMF corresponding to the cation-binding sites are at the extremities of the channel, in agreement with experiment (67, 88, 97). No large free-energy barrier appears to be associated with the dehydration process at the entrance of the pore. In the interior of the pore (see Figure 2), the (L,D) elementary free-energy barriers are on the order of 4.5 kcal/mol for Na^+. Almost half of each barrier is caused by the two neighboring single-file waters and results from a loss of water-peptide hydrogen bonds. The translocation

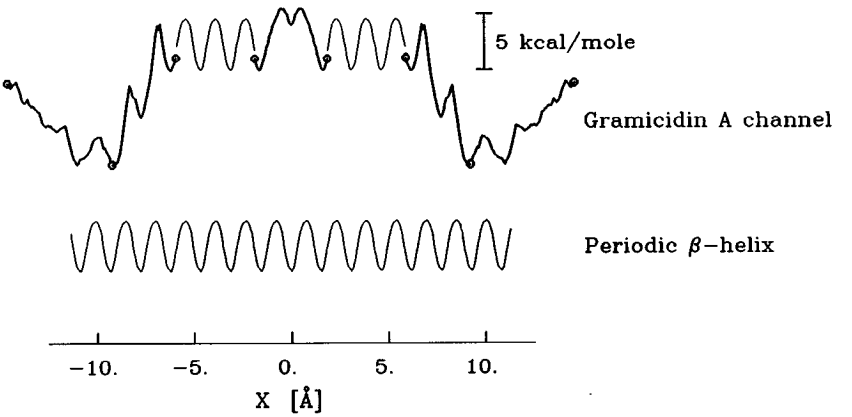

Figure 1 PMF along the gramicidin RK dimer obtained by assembling the three regions considered explicitly in the free-energy calculations (*bold line*) and a connector going from 6.02 to 1.65 Å (*thin line*) constructed from the PMF inside the periodic RK helix (shown at the bottom, see also Figure 2). The position of the connector was adjusted vertically by adding a constant energy term to the periodic PMF to match the values at $x = 6.02$ Å. Its amplitude was not scaled, and the horizontal position was neither adjusted nor scaled. Thus, the distance between the well of the periodic connector is 1.55 Å and the energy barriers are 4.5 kcal/mol as calculated in the periodic β-helix. The vertical position of the intermonomer segment was adjusted so that the energy in the first wells located at ± 1.55 Å is equal to the energy in the fourth wells located at ± 6.02 Å. The lowest energy minima are located at ± 9.30 and ± 11.05 Å corresponding to the Na^+ binding sites. The largest energy barrier is about 8 kcal/mol in the entrance region between wells 5 and 4 located at ± 6.97 Å (taken from Ref. 81 with permission).

Table 1 Position of the free energy minima in the RK-dimer channel

Minima	Residues[a]				Position x (Å)
0	L-Val1′	L-Ala3	L-Ala3′	L-Val1	0.00
1	Formyl	L-Ala5	L-Val1′	L-Ala3	1.65
2[b]	Gly2	L-Ala7	Formyl	L-Ala5	3.10
3[b]	D-Leu4	L-Trp9	Gly^2	L-Ala7	4.65
4	D-Val6	L-Trp11	D-Leu4	L-Trp9	6.17
5	D-Val8	L-Trp13	D-Val6	L-Trp11	7.75
6[c]	D-Leu10	L-Trp15	D-Val8	L-Trp13	9.30
7[c]	D-Leu12	Ethanol	D-Leu10	L-Trp15	11.05

[a] Primed residue numbers belong to the second monomer.
[b] Predicted from the periodic RK β-helix.
[c] Lowest free energy minima and probably the major Na^+ binding sites.

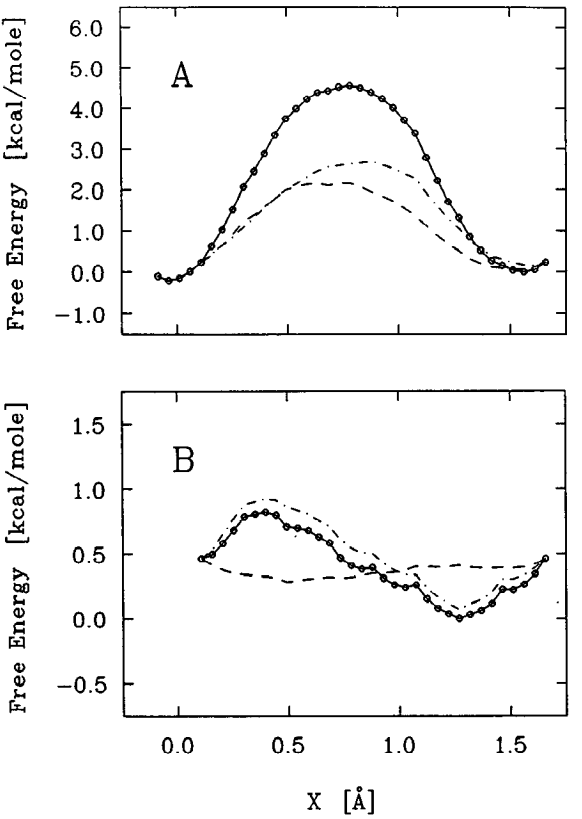

Figure 2 PMF of Na^+ (*A*) and K^+ (*B*) ions in the periodic RK-helix as obtained from the free-energy difference perturbation technique. A hysteresis of 0.8 and 1.0 kcal/mol was corrected for Na^+ and K^+, respectively. Water (*dot-dashed line*) and channel (*dashed line*) contributions to the PMF of Na^+ (*A*) and K^+ (*B*) ions from the mean force decomposition are shown. The PMF in the periodic helix is an approximation to the elementary translocation free-energy barrier for one (L,D) unit in the interior of the dimer channel (taken from Ref. 79, with permission).

proceeds from random hopping transitions, occurring at a rate of about $2.3 \times 10^8\ s^{-1}$, between distinct energy wells. For K^+, the very small (L,D) elementary free-energy barriers, on the order of 1.0 kcal/mol, are due entirely to the waters; the translocation proceeds as a continuous chaotic diffusive motion controlled by the dissipative forces acting on the single-file movements of water.

Although the absolute binding constant for a cation depends on the large ion-water and ion-channel interactions, the elementary translo-

cation barriers in the interior of the pore are not controlled by the large interaction energy involving the ion. Instead they arise from the weaker water-water, water-peptide, and peptide-peptide hydrogen bond interactions. The water molecules make a significant contribution to the free energy of activation (see Figure 2) and to the dissipative forces acting on the ions. Classical transition state theory does not provide an adequate description of the dynamics of ions in the interior of the channel; both Na^+ and K^+ suffer many dissipative damping collisions and their dynamics are chaotic.

It is likely that several of the present conclusions provide a general microscopic picture of the permeation process through narrow single-file molecular pores and are not limited to the gramicidin channel. However, the motion of ions through ATP-driven pumps or pores and larger channels may be governed by other microscopic mechanisms due to differences in the molecular arrangements, water structures, and other pore-specific factors.

The nature of the gramicidin results demonstrates the importance of having information on the structure of the channel prior to investing the time (human and computer) for such simulations. Furthermore, despite the sophistication of modern computational methods, it is important to realize that the simulations have limitations, particularly in studying complex biological systems. Experimentally measured differences in ion permeabilities can often be accounted for by changes of only a few kilocalories per mole in the activation energies. Such small differences are within the uncertainty of present computational methods. The errors of the Born-Openheimer energy surface obtained directly from ab initio quantum chemistry methods, or approximated through a potential energy function, make it very difficult to achieve the accuracy needed for predicting the selectivity of ion channels. Thus, in a theoretical study of ion permeation based on a detailed atomic model, the analysis of the microscopic factors not directly accessible to experimental measurements is of greater interest than the absolute rate.

In a near future, the growing body of experimental data on the properties of modified gramicidin channels will be exploited. Experiments involving amino acid substitutions and chemical modifications will allow the investigation of the influence of particular molecular groups on the permeation process (2, 6, 7) and on the stability of monomer-monomer association in the lipid membrane (6). The gramicidin molecule is particularly well suited for such studies in view of of its structural and functional simplicity. Currently, investigations are underway of the gramicidin channel incorporated in a realistic membrane envi-

ronment, including the bulk water and the surrounding phospholipids (101, 102, 106–108), the thermodynamic factors governing double-ion occupancy (82), and the flickering kinetics of a dioxalone-linked channel (21).

This review demonstrates that modern computational methods, such as molecular dynamics simulations, provide powerful tools for the study of ion transport in complex biological systems. As the three-dimensional structures of biologically relevant channels become available, the theoretical methods outlined in this review should provide a roadmap for studies of the function of such systems. As an example, simulations on the dynamics of porins (20, 104), large pores that have been shown to be β-barrel trimers, are in progress (M Watanabe, J Rosenbusch, T Schirmer & M Karplus, in preparation).

ACKNOWLEDGMENTS

This review was supported in part by a grant from the National Science Foundation to MK. We thank David Busath for supplying a file containing over 700 references.

Literature Cited

1. Andersen OS. 1984. Gramicidin channels. *Annu. Rev. Physiol.* 46:531–48
2. Andersen OS, Koeppe RE II, Durkin JT, Mazet JL. 1987. Structure-function on linear gramicidins: site specific modifications in a membrane channel. See Ref. 109, pp. 295–314
3. Åqvist J, Warshel A. 1989. Energetics of ion permeation through membrane channels. *Biophys. J.* 56:171–82
4. Arseniev AS, Bystrov VF, Ivanov TV, Ovchinnikov YA. 1985. ^{1}H-NMR study of gramicidin-A transmembrane ion channel. Head-to-head right-handed single stranded helices. *FEBS Lett.* 186:168–74
5. Barnes P, Finney JL, Nicholas JD, Quinn JE. 1979. Cooperative effects in simulated water. *Nature* 282:459–64
6. Becker MD, Greathouse DV, Koeppe RE II, Andersen OS. 1991. Amino acid sequence modulation of gramicidin channel function: effects of tryptophane-to-phenylalanine substitutions on the single-channel conductance and duration. *Biochemistry* 30:8830–39
7. Becker MD, Koeppe RE II, Andersen OS. 1992. Amino acid substitution and ion channel function. *Biophys. J.* 62: 25–27
8. Berendsen HJC, Postma JPM, van Gunsteren WF, Hermans J. 1981. Interaction models for water in relation to proteins hydration. In *Intermolecular Forces*, ed. B Pullman, pp. 331–42. Dordrecht: Reidel
9. Berne BJ, Borkovec M, Straub JE. 1988. Classical and modern methods in reaction rate theory. *J. Phys. Chem.* 92:3711–25
10. Born M. 1920. Volumen und hydratationswarme der ionen. *Z. Phys.* 1:45
11. Brooks BR, Bruccoleri RE, Olafson BD, States DJ, Swaminathan S, Karplus M. 1983. CHARMM: a program for macromolecular energy minimization and dynamics calculations. *J.Comput. Chem.* 4:187–217
12. Brooks CL III, Karplus M, Pettitt BM. 1988. Proteins. A theoretical perspective of dynamics, structure and thermodynamics. *Adv. Chem. Phys.* Vol. 71
13. Busath D, Hemsley G, Bridal T, Pear

M, Gaffney K, Karplus M. 1988. Guanidnium as a probe of the gramicidin channel interior. See Ref. 75a, pp. 187–201
14. Chandler D. 1978. Statistical mechanics of isomerization dynamics in liquids and the transition state approximation. *J. Chem. Phys.* 68:2959–70
15. Chiu SW, Gulukota K, Jakobsson E. 1992. Computational approaches to understanding the ion channel-lipid system. In *Proteins: Structures, Interactions, and Models*, ed. A Pullman, B Pullman, J Gortner, pp. 315–38. Dordrect: Kluwer Academic
16. Chiu SW, Jakobsson E, Subramaniam S, McCammon JA. 1991. Time-correlation analysis of simulated water motion in flexible and rigid gramicidin channels. *Biophys. J.* 60:273–85
17. Chiu SW, Nicholson LK, Brenneman MT, Subramaniam S, Teng Q, et al. 1991. Molecular dynamics computations and solid state state NMR of the gramicidin cation channel. *Biophys. J.* 60:974–78
18. Chiu SW, Novotny JA, Jakobsson E. 1993. The nature of ion and water barrier crossings in a simulated ion channel. *Biophys. J.* 64:98–108.
19. Chiu SW, Subramaniam S, Jakobsson E, McCammon JA. 1989. Water and polypeptide conformations in the gramicidin channel. *Biophys. J.* 56: 253–61
20. Cowan SW, Schirmer T, Rummel G, Steiert M, Ghosh R, et al. 1992. Crystal structures explain functional properties of two *E. coli* porins. *Nature* 358: 727
21. Crouzy S, Woolf T, Roux B. 1992. Molecular dynamics exploration of gating in dioxolae ring linked gramicidin. *Biophys. J.* 61:A525
22. Eisenman G, Horn R. 1983. Ionic selectivity revisited: the role of kinetic and equilibrium processes in ion permeation through channels. *J. Membr. Biol.* 76:197–225
23. Etchebest C, Pullman A. 1985. The effect of the amino-acid side chains on the energy profiles for ion transport in the gramicidin A channel. *J. Biomol. Struct. Dyn.* 2:859–70
24. Etchebest C, Pullman A. 1986. The gramicidin A channel: energetics and structural characteristics of the progression of a sodium ion in the presence of water. *J. Biomol. Struct. Dyn.* 3:805–25
25. Etchebest C, Pullman A. 1986. The gramicidin-A channel—the energy profile calculated for Na^+ in the presence of water with inclusion of the flexibility of the ethanolamine tail. *FEBS Lett.* 204:261–65
26. Etchebest C, Pullman A. 1988. The gramicidin A channel: left versus right-handed helix. See Ref. 75a, pp. 167–85
27. Etchebest C, Pullman A. 1988. Energy profile of Cs^+ in gramicidin A in the presence of water. Problem of the ion selectivity of the channel. *J. Biomol. Struct. Dyn.* 5:1111–25
28. Etchebest C, Pullman A, Ranganathan S. 1984. The gramicidin A channel: comparison of the energy profiles of Na^+, K^+ and Cs^+. Influence of the flexibility of the ethanolamine end chain on the profiles. *FEBS Lett.* 173: 301–6
29. Etchebest C, Pullman A, Ranganathan S. 1985. The gramicidin A channel: theoretical energy profile computed for single occupancy by a divalent cation Ca^{2+}. *Biochim. Biophys. Acta* 818:23–30
30. Fischer W, Brickmann J, Läuger P. 1981. Molecular dynamics study of ion transport in transmembrane protein channels. *Biophys. Chem.* 13:105–16
31. Fornili SL, Vercauteren DP, Clementi E. 1984. Water structure in the gramicidin A transmembrane channel. *Biochim. Biophys. Acta* 771:151–64
32. Gilson MK, Honig B. 1988. Calculation of the total electrostatic energy of a macromolecular system. *Protein* 4: 7–18
33. Gresh N, Claverie P, Pullman A. 1979. Intermolecular interactions: reproduction of the results of *ab initio* supermolecule computations by an additive procedure. *Int. J. Quant. Chem.* 13: 243–53
34. Heitz F, Daumas P, Van Mau N, Lazaro R, Trudelle Y, Etchebest C, Pullman A. 1988. Linear gramicidins: influence of the nature of the aromatic side chains on the channel conductance. See Ref. 75a, pp. 167–85
35. Hinton JF, Fernandez JQ, Shungu DC, Whaley WL, Koeppe RE II, Millett FS. 1988. Tl-205 nuclear magnetic resonance determination of the thermodynamic parameters for the binding of monovalent cations to Gramicidin A and C. *Biophys. J.* 54:527–33
36. Hirata F, Redfern P, Levy RM. 1988. Viewing the born model for ion hydration through a microscope. *Int. J. Quant. Chem. Quant. Biol. Symp.* 15: 179–90

37. Hladky SB, Haydon DA. 1984. Ion movements in gramicidin channels. *Curr. Top. Membr. Transp.* 21:327–72
38. Deleted in proof
39. Jayaram B, Fine R, Sharp K, Honig B. 1989. Free energy calculations of ion hydration: an analysis of the born model in terms of microscopic simulations. *J. Phys. Chem.* 93:4320–27
40. Jordan PC. 1984. The total electrostatic potential in a gramicidin channel. *J. Membr. Biol.* 78:91–102
41. Jordan PC. 1987. Microscopic approach to ion transport through transmembrane channels. The model system gramicidin. *J. Phys. Chem.* 91: 6582–91
42. Jordan PC. 1988. Ion transport through transmembrane channels: ab initio perspectives. *Curr. Top. Membr. Transp.* 33:91–111
43. Jordan PC. 1988. A molecular dynamics study of cesium ion motion in a gramicidin-like channel. See Ref. 75a, pp. 237–51
44. Jordan PC. 1990. Ion-water and ion-polypeptide correlations in a gramicidin-like channel. A molecular dynamics study. *Biophys. J.* 58:1133–56
45. Jorgensen WL, Chandrasekhar J, Madura JD, Impey RW, Klein ML. 1983. Comparison of simple potential functions for simulating liquid water. *J. Chem. Phys.* 79:926–35
46. Kebarle P. 1977. Ion thermochemistry and solvation from gas phase ion equilibria. *Annu. Rev. Phys. Chem.* 28: 445–76
47. Kebarle P, Caldwell C, Magnera T, Sunner J. 1985. Ion-gas phases and solution-dipolar aprotic solvents. *Pure Appl. Chem.* 57:339–46
48. Kim KS. 1985. Microscopic effect of an applied voltage on the solvated gramicidin A transmembrane channel in the presence of Na^+ and K^+ cations. *J. Comp. Chem.* 6:256–63
49. Kim KS, Clementi E. 1985. Energetics and hydration structure of a solvated gramicidin A channel for K^+ and Na^+ cations. *J. Am. Chem. Soc.* 107:5504–13
50. Kim KS, Vercauteren DP, Welti M, Chin S, Clementi E. 1985. Interaction of K^+ ion with the solvated gramicidin A transmembrane channel. *Biophys. J.* 47:327–35
51. Kirkwood JG. 1935. Statistical mechanics of fluid mixtures. *J. Chem. Phys.* 3:300
52. Koeppe RE II, Kimura M. 1984. Computer building of β-helical polypeptide models. *Biopolymers* 23:23–38
53. Läuger P. 1973. Ion transport through pores: a rate theory analysis. *Biochim. Biophys. Acta* 311:423–41
54. Läuger P. 1982. Microscopic calculation of ion-transport rates in membrane channels. *Biophys. Chem.* 15:89–100
55. Lee S, Karplus M. 1984. Brownian dynamics simulation: statistical error of correlation functions. *J. Chem. Phys.* 81:6106–18
56. Lee WK, Jordan PC. 1984. Molecular dynamics simulation of cation motion in water-filled gramicidin-like pores. *Biophys. J.* 46:805–19
57. Levitt DG. 1986. Interpretation of biological channel flux data—reaction-rate theory versus continuum theory. *Annu. Rev. Biophys. Biophys. Chem.* 15:29–57
58. Mackay DH, Berens PH, Wilson KR, Hagler AT. 1984. Structure and dynamics of ion transport through gramicidin A. *Biophys. J.* 46:229–48
59. Mackay DH, Wilson KR. 1986. Possible allosteric significance of water structures in proteins. *J. Biomol. Struct. Dyn.* 4:491–500
60. Matsuoka O, Clementi E, Yoshimine M. 1976. CI study of the water dimer potential surface. *J. Chem. Phys.* 64: 1351–61
61. Mazor M, Pettitt MB. 1991. Convergence of the chemical potential in aqueous simulations. *Mol. Simul.* 6:1
62. McCammon JA, Gelin BR, Karplus M. 1977. Dynamics of folded proteins. *Nature* 267:585–90
63. Momany FA, McGuire RF, Burgess AW, Scheraga HA. 1975. Energy parameters in polypeptides vii. *J. Chem. Phys.* 79:2361–81
64. Monoi H. 1993. Energy-minimized conformation of gramicidin-like channels. I. Infinitely long poly (L,D)-alanine $\beta^{6.3}$-helix. *Biophys. J.* 64:36–43
65. Naik VM, Krimm S. 1986. Vibrational analysis of the structure of gramicidin A. 1. Normal mode analysis. *Biophys. J.* 49:1131–45
66. Nicholson LK, Cross TA. 1989. The gramicidin cation channel: an experimental determination of the right-handed helix sense and verification of β-type hydrogen bonding. *Biochemistry* 28:9379–85
67. Olah GA, Huang HW, Liu W, Wu Y. 1991. Location of ion-binding sites in the gramicidin channel by X-ray diffraction. *J. Mol. Biol.* 218:847–58
68. Parsegian A. 1969. Energy of an ion

crossing a low dielectric membrane: solution to four relevant electrostatic problems. *Nature* 221:844–46

68a. Parsegian VA, ed. 1984. *Ionic Channels in Membranes. Biophysical Discussions*. New York: Rockefeller Univ. Press

69. Partenskii MB, Jordan PC. 1992. Nonlinear dielectric behavior of water in transmembrane ion channels: ion energy barriers and the channel dielectric constant. *J. Phys. Chem.* 96:3906–10

70. Patey GN, Valeau JP. 1975. A Monte Carlo method for obtaining the interionic potential of mean force in ionic solution. *J. Chem. Phys.* 63:2334–39

71. Pettitt BM, Rossky PJ. 1986. Alkali halides in water: ion-solvent and ion-ion potential of mean force at infinite dilution. *J. Chem. Phys.* 84:5836–44

72. Polymeropoulos EE, Brickmann J. 1985. Molecular dynamics of ion transport through transmembrane model channels. *Annu. Rev. Biophys. Biophys. Chem.* 14:315–30

73. Pullman A. 1987. Energy profiles in the gramicidin A channel. *Q. Rev. Biophys.* 20:173–200

74. Pullman A, Etchebest C. 1983. The gramicidin A channel: the energy profile for single and double occupancy in a head-to-head beta(6.3 3,3)-helical dimer backbone. *FEBS Lett.* 163:199–202

75. Pullman A, Etchebest C. 1987. The effect of molecular structure and of water on the energy profiles in the gramicidin A channel. See Ref. 109, pp. 277–93

75a. Pullman A, Gortner J, Pullman B, eds. 1988. *Transport Through Membranes: Carriers Channels and Pumps*. Boston: Kluwer Academic

76. Roux B. 1993. Theory of transport in ion channels: from molecular dynamics simulations to experiments. In *Computer Simulation in Molecular Biology*, ed. J Goodefellow. Weinheim: VCH. In press

77. Roux B. 1993. Nonadditivity in cation-peptide interactions: a molecular dynamics and ab initio study of Na^+ in the gramicidin channel. *Chem. Phys. Lett.* 212:231–40

78. Roux B, Karplus M. 1988. The normal modes of the Gramicidin A dimer channel. *Biophys. J.* 53:297–309

79. Roux B, Karplus M. 1991. Ion transport in a gramicidin-like channel: structure and thermodynamics. *Biophys. J.* 59:961–81

80. Roux B, Karplus M. 1991. Ion transport in a gramicidin-like channel: dynamics and mobility. *J. Phys. Chem.* 95:4856–68

81. Roux B, Karplus M. 1993. Ion transport in the gramicidin channel: free energy of the solvated right-handed dimer in a model membrane. *J. Am. Chem. Soc.* 115:3250–60

82. Roux B, Karplus M. 1993. Double ion occupancy in the gramicidin channel: a molecular dynamics study. *Biophys. J.* 64:A354

83. Roux B, Yu HA, Karplus M. 1990. Molecular basis for the born model of ion solvation. *J. Phys. Chem.* 94:4683–88

84. Schlenkrich M, Bopp Ph, Skerra A, Brickmann J. 1988. Structure and dynamics of water on membrane surfaces and in narrow transmembrane channels—molecular dynamics simulations. See Ref. 75a, pp. 219–235

85. Schroeder H, Brickmann J, Fischer W. 1983. Cation transport through biological transmembrane channels. Theoretical study of mass dependent anomalies in the diffusion constant. *Mol. Phys.* 49:973–79

86. Skerra A, Brickmann J. 1987. Structure and dynamics of one-dimensional ionic solutions in biological transmembrane channels. *Biophys. J.* 51:969–76

87. Skerra A, Brickmann J. 1987. Simulation of voltage-driven hydrated cation transport through narrow transmembrane channels. *Biophys. J.* 51: 977–83

88. Smith R, Thomas DE, Atkins AR, Separovic F, Cornell BA. 1990. Solid-state ^{13}C-NMR studies of the effects of sodium ions on the gramicidin A ion channel. *Biochim. Biophys. Acta* 1026: 161–66

89. Smith R, Thomas DE, Separovic F, Atkins AR, Cornell BA. 1989. Determination of the structure of a membrane-incorporated ion channel. *Biophys. J.* 56:307–14

90. Stanley RH, Beauchamp JL. 1975. Intrinsic acid-base properties of molecules. Binding of Li^+ to π- and n-donor bases. *J. Am. Chem. Soc.* 97:5920–21

91. Sung SS, Jordan PC. 1987. The interaction of Cl^- with a gramicidin-like channel. *Biophys. Chem.* 27:1–6

92. Sung SS, Jordan PC. 1987. Why is gramicidin valence selective? A theoretical study. *Biophys. J.* 51:661–72

93. Sung SS, Jordan PC. 1988. Theoretical study of the antiparallel double-

stranded helical dimer of gramicidin as an ion channel. *Biophys. J.* 54:510–26
94. Sung SS, Jordan PC. 1989. The channel properties of possible gramicidin dimers. *J. Theor. Biol.* 140:369–80
95. Turano B, Pear M, Busath D. 1992. Gramicidin channel selectivity. Molecular mechanics for formamidinium, guanidinium and acetamididium. *Biophys. J.* 63:152–61
96. Urry DW. 1971. The gramicidin A transmembrane channel: a proposed π_{LD} helix. *Proc. Natl. Acad. Sci. USA* 68:672–76
97. Urry DW, Trapane TL, Prasad KU. 1983. Is the gramicidin A transmembrane channel single-stranded or double stranded helix? A simple unequivocal determination. *Science* 221:1064–67
98. Urry DW, Venkatachalam CM. 1983. Theoretical conformation analysis of the gramicidin A transmembrane channel. I. Helix sense and the energetics of head-to-head dimerization. *J. Comp. Chem.* 4:461–69
99. Urry DW, Venkatachalam CM, Prasad KU, Bradley RJ, Parenti-Castelli G, Lenaz G. 1981. Conduction process of the gramicidin channel. *Int. J. Quant. Chem. Quant. Biol. Symp.* 8:385–99
100. Urry DW, Venkatachalam CM. 1984. Theoretical conformation analysis of the gramicidin A transmembrane channel. II. Energetics of helical states of the channel. *J. Comp. Chem.* 5:64–71
100a. van Gunsteren WF, Berendsen HJC. 1987. Biomos. *Nijenborgh* Vol. 16
101. Wang J, Pullman A. 1990. The intrinsic molecular potential of glyceryl monooleate layers and its effect on the conformation and orientation of an inserted molecule: example of gramicidin A. *Biochim. Biophys. Acta* 1024:10–18
102. Wang J, Pullman A. 1991. Interactions and packing of lipids around a helical hydrophobic polypeptide—the system gramicidin-A glycerylmonooleate. *Chem. Phys. Lipids* 57:1–16
103. Warshel A, Levitt M. 1976. Theoretical studies of enzymatic reactions: dielectric, electrostatic and steric stabilization of the cabonium ion in the reaction of lysozyme. *J. Mol. Biol.* 103:2218–24
104. Weiss MS, Abele U, Weckesser J, Welte W, Schiltz E, Schulz GE. 1991. Molecular architecture and electrostatic properties of a bacterial porin. *Science* 254:1627
105. Wooley GA, Wallace BA. 1992. Model ion channels: gramicidin and alamethecin. *J. Membr. Biol.* 129:109–36
106. Woolf TB, Roux B. 1993. Molecular dynamics of proteins in lipid membranes: the first steps. *Biophys. J.* 64: A354
107. Xing J, Scott HL. 1989. Monte Carlo studies of lipid chains and gramicidin A in a model membrane. *Biophys. Biochem. Res. Commun.* 165:1–6
108. Xing J, Scott HL. 1992. Monte Carlo studies of a model for lipid-gramicidin A bilayers. *Biochim. Biophys. Acta* 1106:227–32
109. Yagi K, Pullman B, eds. 1987. *Ion Transport Through Membranes*. Boston: Kluwer Academic

Annual Review of Biophysics and Biomolecular Structure
Volume 23, 1994

CONTENTS

vi (*continued*)

DYNAMICS

EMERGING TECHNIQUES